

Improving the performance of double-plane stereo vision system calibration, using a virtual plane

Paweł Rotter, Witold Byrski,
Michał Dajda, Grzegorz Łojek

AGH – University of Science and Technology,
Automatics Department,
Kraków, Poland

Received 17 May 2010

Accepted 19 July 2010

Abstract

In the double-plane method for stereo vision system calibration, the correspondence between screen coordinates and location in 3D space is calculated based on four plane-to-plane transformations; there are two planes of the calibration pattern and two cameras. The method is intuitive, and easy to implement, but, the main disadvantage is ill-conditioning for some spatial locations. In this paper we propose a method which exploits the third plane which physically does not belong to the calibration pattern, but can be calculated from the set of reference points. Our algorithm uses a combination of three calibration planes, with weights which depend on screen coordinates of the point of interest; a pair of planes which could cause numerical errors receives small weights and have practically no influence on the final results. We analyse errors, and their distribution in 3D space, for the basic and the improved algorithm. Experiments demonstrate high accuracy and reliability of our method compared to the basic version; root mean square error and maximum error, are reduced by factors of 4 and 20 respectively.

Keywords

stereo vision · camera calibration · double-plane method

1. Introduction

Calibration of a stereo vision system is a process of finding the correspondence between coordinates of points in 3-dimensional space, and 2-dimensional coordinates of the corresponding points at the screen planes of cameras. Parameters of the calibration transform implicitly include both internal parameters of the camera (such as focal length) and external parameters, related to the position of the camera in the external coordinate system.

Calibration of stereo vision systems is usually performed by the use of a calibration pattern, which is a 3-dimensional object with known metric structure. In classical calibration in 3D space, the calibration pattern consists of a minimum of 6 points, and each of them generates 2 equations. 11 parameters of the transformation are calculated by solving the system of at least 11 equations, usually with the SVD method [2, 4].

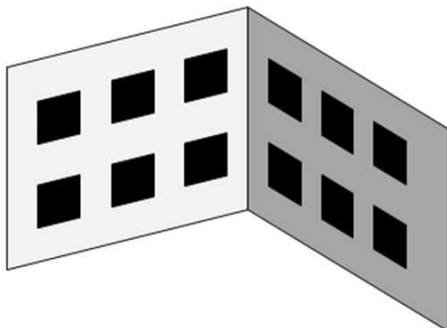


Figure 1. An example of calibration pattern.

In the method which we hereby propose, the problem is decomposed into two projections from 2-dimensional planes to the screen planes. The idea of using two plane-to-screen transformations for camera calibration in 3D space, the so called *double-plane method*¹, was presented by Drenk et al. [3] and by Zhang [10]. The calibration pattern includes two sets of points, located on two parallel planes. Coordinates of a point M in 3D space observed by two cameras can be found by calculation of the intersection point of two lines, as shown in Figure 2.

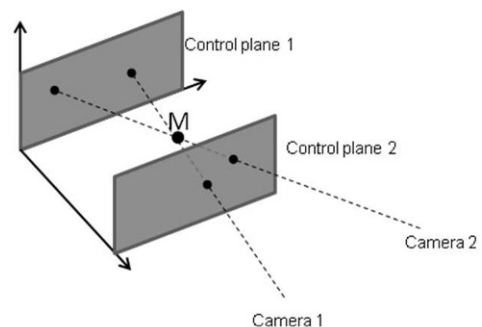


Figure 2. Double plane method with parallel planes.

Application of two control planes instead of one 3D calibration pattern has some advantages. A complex problem is decomposed into two

¹ <http://www.kwon3d.com/theory/dlt/doub.html>

tasks with smaller complexity. The method and its geometric interpretation are very intuitive.

On the other hand, in practical applications, it is often more convenient to use a calibration pattern formed by two perpendicular planes, for example a classical calibration pattern such as that shown in Figure 1. This kind of pattern more easily fits objects of real scenes such as walls, tables, etc. In the double-plane method, the shape and possible obstruction of one plane by another makes the calibration less practical. If perpendicular planes were used in the double-plane method, the shape of the calibration pattern could be the same as in the classical methods, and the minimal number of control points could be reduced from 8 to 6; two control points can be common to both control planes. However, intersection of the control planes raises a problem at the stage of 3D space reconstruction, coordinates of points which are seen by any camera at the intersection line cannot be calculated properly.

In all the calibration methods which rely on any plane-based calibration pattern, ill-conditioning may occur for some points. In monographs on stereo vision, the problem of ill-conditioning of the calibration is usually not discussed in detail [1, 2, 8]; moreover, it requires a dedicated analysis for each calibration method. Among over 170 papers on camera calibration listed at <http://www.visionbib.com/bibliography/active672.html> only a few refer to this problem. Methods for avoidance of singularities for some specific calibration algorithms were studied by Sturm and Maybank [8] and Zhang [11].

In this article we propose a method for singularity avoidance for double-plane calibration with perpendicular calibration planes. Singularities may be observed for points which are seen by any camera at the intersection line. Our method uses the configuration of 6 reference points at two perpendicular planes Π_1 and Π_2 , such that a third plane Π_3 can be calculated without the need for additional reference points (see Figure 3). Our algorithm adjusts the combination of planes Π_1 , Π_2 and Π_3 used for calculations, in order to reduce errors resulting from proximity of the intersection line, and to ensure continuity of the stereo transformation.

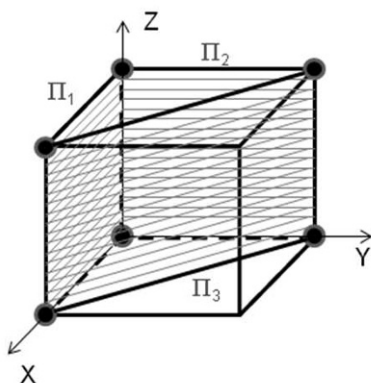


Figure 3. In our method location of the reference points at planes Π_1 and Π_2 facilitates calculation of the third plane Π_3 .

2. Basic algorithm: using two perpendicular calibration planes

The basic version of the algorithm consists of four 2D homographies. Let us recall that 2D homography is a transformation which describes perspective projection from one 2D plane to another, in our case from the plane of the calibration pattern, to the plane of CCD matrix (or to the plane of the screen – transformation between the CCD plane and the screen plane can be included in projection parameters) – see Figure 4. More generally, transformation H may include a superposition of any number of intermediate plane-to-plane homographies. Transformation H includes all the information about optical parameters of the camera, with the assumption that they are linear. The most important nonlinearities are radial distortions – the algorithm for their compensation is presented in [7], chapter 2.1.4. In most applications however, cameras are assumed to be linear.

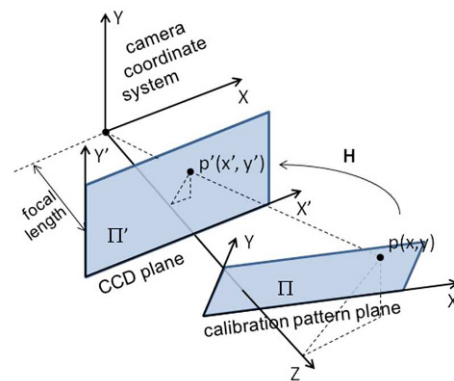


Figure 4. 2D homography.

In order to calibrate the system, i.e., to find the transformation H, coordinates of at least four points in the plane Π (no 3 of which can be collinear) and their projections to the plane Π' are needed. The solution can be found using the Direct Linear Transformation (DLT) algorithm, see e.g. [6], chapter 4.1.

In the basic version of the algorithm, originally published in [5], the stereo vision system of two cameras is calibrated using two planar 4-tuples of reference points. Two points may be common in both planes, so the calibration pattern can be made of 6 points, for example six vertices of the cube, selected as shown in Figure 5.

In this example, the choice of planes $\Pi_1=XZ$ and $\Pi_2=YZ$ facilitates the conversion between local systems (XZ and YZ) and the global system XYZ. Calibration of the system consists of the calculation of four vectors $p(C_i, \Pi_j)$, and the calibration parameters for the camera C_i and the plane Π_j , where $i, j \in \{1,2\}$. The algorithm for reconstruction of 3D coordinates is presented below. Vectors $p_{C1} = (x_{C1}, y_{C1})$ and $p_{C2} = (x_{C2}, y_{C2})$ are coordinates of the same point of 3D space in screen coordinate system of the camera 1 and camera 2 respectively.

Algorithm 1. Basic method for 3D coordinates reconstruction

Step 1 Calculation of the projections of points p_{C1} and p_{C2} onto planes Π_1 and Π_2 : $p_{C1\Pi1}, p_{C1\Pi2}, p_{C2\Pi1}, p_{C2\Pi2}$.

Step 2 Conversion of the coordinates of points $p_{C1\Pi1}, p_{C1\Pi2}, p_{C2\Pi1}, p_{C2\Pi2}$.

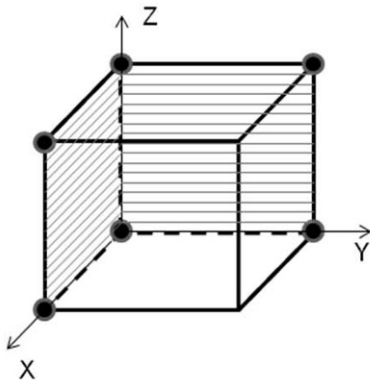


Figure 5. An example of the calibration points choice.

$p_{C2\Pi2}$, from local 2D coordinate systems to the global 3D coordinate system.

Step 3 Calculation of two straight lines: $l_1 = (p_{C1\Pi1}, p_{C1\Pi2})$ and $l_2 = (p_{C2\Pi1}, p_{C2\Pi2})$.

Step 4 Calculation of the common point of l_1 and l_2 : $p = l_1 \cap l_2$. In practice, due to limited precision and space discretization, l_1 and l_2 are close to each other, but usually do not have a common point; thus, p is calculated as the middle of the shortest section which joins l_1 and l_2 .

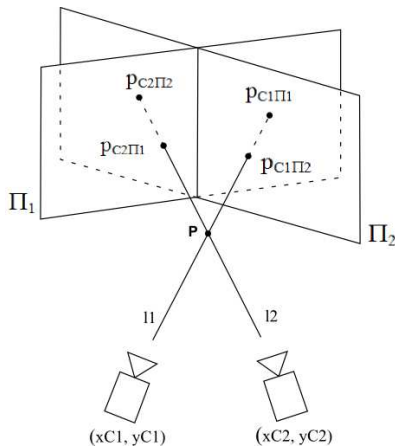


Figure 6. Reconstruction of 3D space in double-plane method is based on four plane-to-plane projections.

3. Improved algorithm: using virtual calibration plane

In the double-plane transformation method, 3D coordinates can be found based on the intersection of two straight lines which join the cam-

eras with the point of interest. The lines are calculated based on points $p_{C1\Pi1}$, $p_{C1\Pi2}$, $p_{C2\Pi1}$, $p_{C2\Pi2}$, as described in step 3. However if one of these lines intersects planes Π_1 and Π_2 at the same point (i.e., at the intersection $\Pi_1 \cap \Pi_2$), two points have the same coordinates and further line calculation is not possible – see Figure 7. Further, if one of lines (l_1 or l_2) is close to $\Pi_1 \cap \Pi_2$, the problem is ill-conditioned and numerical errors occur.

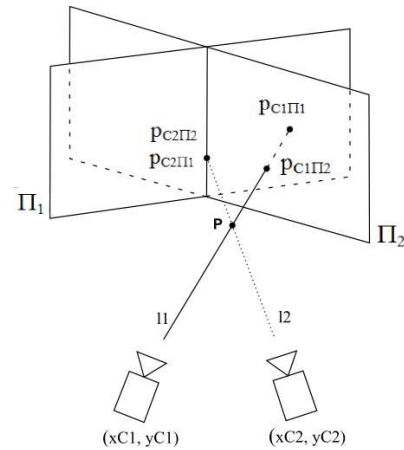


Figure 7. Reconstruction of coordinates for points which are seen by one of the cameras close to the intersection line of control planes. Line l_2 can't be calculated.

If the reference points of the calibration pattern are located as shown in Figure 3, the third virtual plane Π_3 can be calculated. We propose to use all three planes in order to reduce numerical errors. At the calibration stage six vectors $\rho(C_i, \Pi_j)$ are calculated, as there are two cameras and three planes. The improved algorithm is presented below.

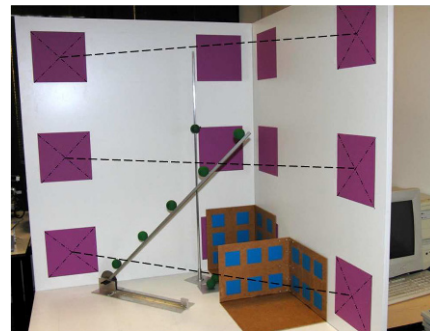


Figure 8. Location of control points in our calibration pattern allows to define the third, virtual plane Π_3 , indicated by three dashed lines.

Algorithm 2. Improved method for 3D coordinates reconstruction

Step 1 Calculation of the projections of points p_{C1} and p_{C2} onto planes Π_1 , Π_2 and Π_3 : $p_{C1\Pi1}$, $p_{C1\Pi2}$, $p_{C1\Pi3}$, $p_{C2\Pi1}$, $p_{C2\Pi2}$, $p_{C2\Pi3}$.

Step 2 Conversion of the coordinates of the points $p_{C1\Pi1}$, $p_{C1\Pi2}$, $p_{C1\Pi3}$, $p_{C2\Pi1}$, $p_{C2\Pi2}$, and $p_{C2\Pi3}$ from local coordinate systems

on the planes Π_1 , Π_2 , and Π_3 to the global 3D coordinate system.

Step 3 Calculation of distances d_i between points $p_{C1\Pi_i}$ and $p_{C2\Pi_i}$ where $i \in \{1,2,3\}$.

Step 4 Calculation of three straight lines: $l_i = (p_{C1\Pi_i}, p_{C2\Pi_i})$ where $i \in \{1,2,3\}$ provided d_i is greater than zero.

Step 5 Calculation of the common points for possible pairs of lines: $p_{12} = l_1 \cap l_2$, $p_{13} = l_1 \cap l_3$, $p_{23} = l_2 \cap l_3$ (see remark in Algorithm 1, Step 4) and corresponding weights w_{12} , w_{13} , w_{23} , where w_{ij} is a square root of $\min\{d_i, d_j\}$.

Step 6 Calculation of the coordinates of the final point as a weighted mean of points p_{12} , p_{13} , p_{23} using weights w_{12} , w_{13} , w_{23} .

4. Experiments

In order to measure the accuracy and compare the proposed algorithm with the basic version we conducted a series of experiments. The calibration pattern was a cube $1\text{ m} \times 1\text{ m} \times 1\text{ m}$, with the control points located to allow the third plane to be defined, as shown in Figure 8.

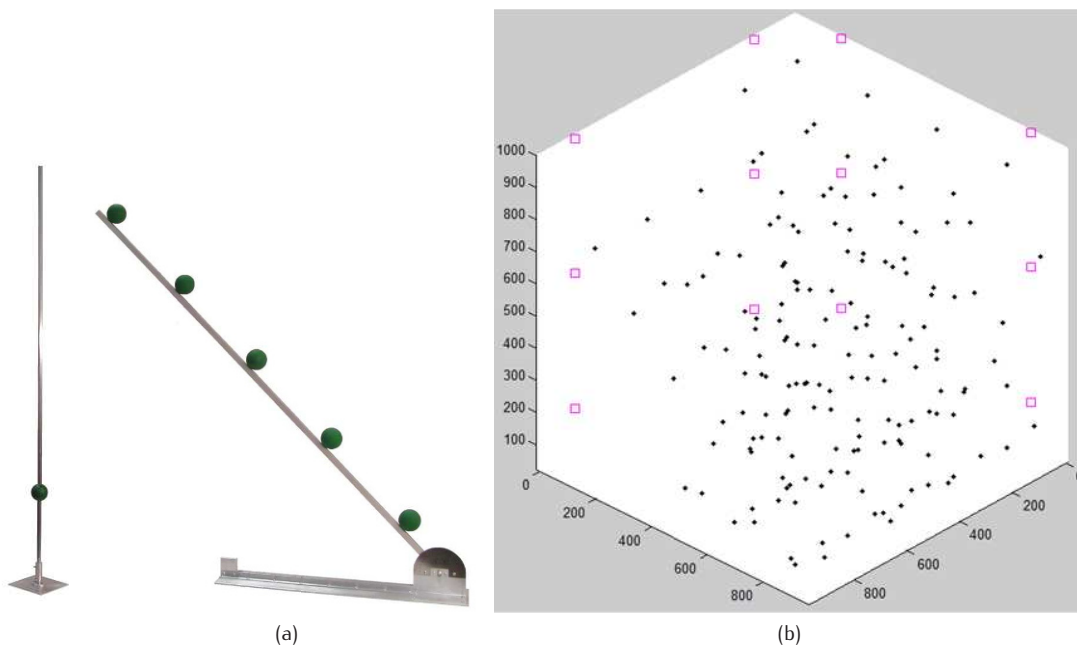


Figure 9. Tools used for precise definition of test points (a) and test points distribution (b)

We used 162 test points with known coordinates, distributed approximately uniformly in the working area (Figure 9(b)). We took high resolution (2816×2112) pictures of these points for 5 different camera setups, which gave us 810 test points in total. For each stereo-pair we calculated the coordinates of each test point using both algorithms, and calculated the error between them and the actual coordinates. Some statistical analysis of the errors is shown in Table 1 and Figure 10 (error δ_i is the Euclidean distance between the calculated and actual location of i -th test point).

The results demonstrate that root mean square error was reduced by close to a factor of 4. More important however, is the fact that singularities, the reason for unreliable results using the basic algorithm, were eliminated (indicated by the reduction of the maximum error by a factor

greater than 20).

To analyse the relationship between the location of points in space, and the errors of both algorithms, we will focus on one of the test series. Location of the cameras and scene for the chosen series is shown in Figure 11(a). As was expected, incorrect results were yielded by the basic algorithm for points near the plane intersection line, and this problem has been eliminated in the improved method. Occasionally exceptions to this finding may be observed, even in close proximity to the plane intersection line. This is the result of randomness of errors: for some relatively small fraction of points, the solution given by an ill conditioned equation is, by coincidence, close to the correct one. Statistical measures for chosen test series are shown in Table 2 and Figure 12.

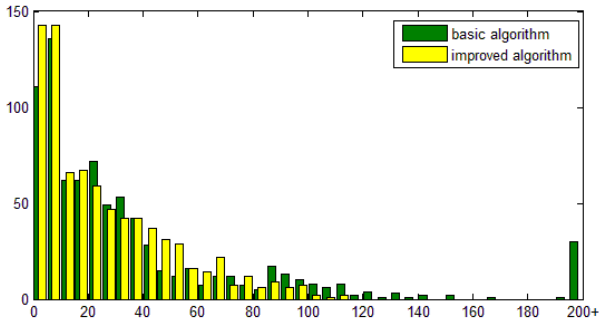


Figure 10. Histograms of errors of the basic and improved algorithm for all test series.

Table 1. Comparison of statistical measures for errors of the basic and improved algorithms, for all test series.

Error measure	Formula	Basic algorithm	Improved algorithm
Maximum error [mm]	$\max_i \delta_i$	2401	115
Mean error [mm]	$\frac{1}{N} \sum_{i=1}^N \delta_i$	49	26
RMSE [mm]	$\frac{1}{N} \sum_{i=1}^N \delta_i^2$	139	36
Median error [mm]	$\text{med } \delta_i$	23	19
Ratio 99 th to 1 st percentile $P_{99}(\delta)/P_{01}(\delta)$		245	45

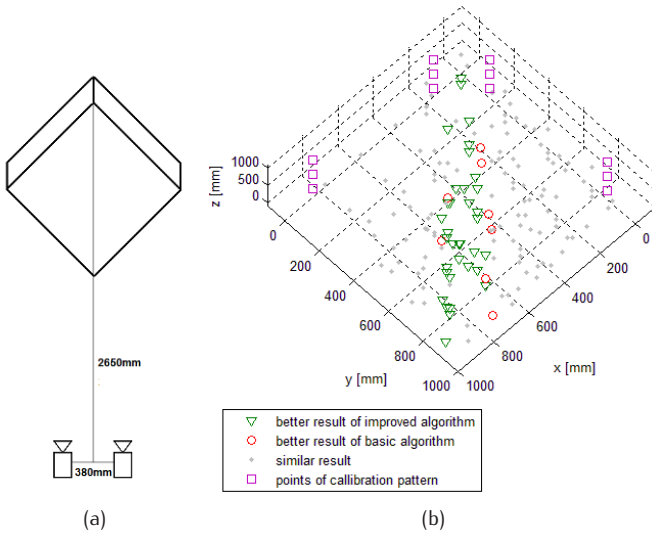


Figure 11. a) Scheme of cameras setup in chosen test series. b) Reconstruction of the scene with marked all test point for chosen test series. Points with error difference between basic and improved algorithm bigger than 10 mm are marked as triangles or circles (differences below 10 mm are presented as similar in order to keep the picture clear).

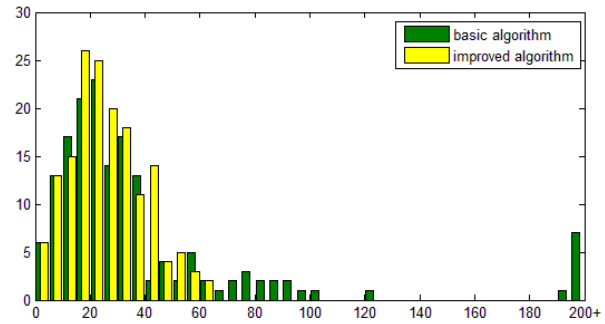


Figure 12. Histograms of errors of basic and improved algorithm for the chosen test series.

calibration planes. Fields in two planes of the calibration pattern allow for calculation of the third, virtual calibration plane which is used for reduction of ill-conditioning of the problem. We analysed errors and their distribution in 3D space for the basic and the improved algorithm for over 800 reference points. Maximum errors, which occur in the basic algorithm due to singularities, were reduced by over a factor of 20, and the root mean square error by a factor approaching 4. The proposed algorithm is intuitive and easy to implement.

As expected, the performance improvement was particularly relevant for points located in proximity to lines connecting cameras with the plane intersection line. Projections of these points to planes Π_1 and Π_2 are close to each other, and there is high probability that numerical errors occur when using the basic algorithm. In the improved algorithm, the 3D coordinates are calculated as a weighted mean of three points, and, in such a case the weight corresponding to point p_{12} is small, thus the influence of numerical errors is reduced.

5. Conclusions

In this paper we proposed a method for the calibration of stereo vision systems which use plane-to-plane transformations with perpendicular

Table 2. Comparison of statistical parameters for errors of basic and improved algorithm for chosen test series.

Error measure	Formula	Basic algorithm	Improved algorithm
Maximum error [mm]	$\max_i \delta_i$	2401	64
Mean error [mm]	$\frac{1}{N} \sum_{i=1}^N \delta_i$	59	26
RMSE [mm]	$\frac{1}{N} \sum_{i=1}^N \delta_i^2$	207	29
Median error [mm]	$\text{med } \delta_i$	25	24
Ratio 99 th to 1 st percentile $P_{99}(\delta)/P_{01}(\delta)$		124	17

References

- [1] A. Bhatti (Ed.) Stereo Vision InTech 2008. Free access at: <http://intechweb.org/book.php?id=87>.
- [2] B. Cyganek, J.P. Siebert An Introduction to 3D Computer Vision Techniques and Algorithms. Wiley 2009.
- [3] V. Drenk, F. Hildebrand, M. Kindler & D. Kliche (1999). A 3D video technique for analysis of swimming in a flume. In R.H. Sanders, & B.J. Gibson (eds.), Scientific Proceedings of the XVII International Symposium on Biomechanics in Sports (pp. 361-364). Perth, Australia: Edith-Cowan University.
- [4] O. Faugeras Three-Dimensional Computer Vision: A Geometric Viewpoint, MIT Press, 1993.
- [5] S. Fuksa, W. Byrski Czteropunktowa metoda identyfikacji transformacji stereowizyjnej (Four-point identification method of stereo-vision transformation) Automatyka 2005, 9(3).
- [6] R. Hartley, A. Zisserman Multiple View Geometry in Computer Vision. Cambridge University Press, 2003.
- [7] R. Klette, K. Schluns, A. Koschan Computer Vision: Three-Dimensional Data from Images. Springer-Verlag, 1998.
- [8] P.F. Sturm, S.J. Maybank On Plane-Based Camera Calibration: A General Algorithm, Singularities, Applications, CVPR, vol. 1, pp.1432, 1999 IEEE Computer Society Conference on Computer Vision and Pattern Recognition (CVPR'99) - Volume 1, 1999.
- [9] A.V. Trucco Introductory Techniques for 3-D Computer Vision, Prentice Hall 1998.
- [10] Z. Zhang A flexible new technique for camera calibration. IEEE Transactions on PAMI, Volume 22, Issue 11, Nov 2000, pp. 1330–1334.
- [11] Z.Y. Zhang Flexible Camera Calibration by Viewing a Plane from Unknown Orientations, ICCV99(666-673), 1999. IEEE DOI Link BibRef 9900.